

# Redox Kinetics of Chini-Type Platinum Carbonyl Clusters Studied by Time-Resolved Pulse Radiolysis

Mona Treguer, Hynd Remita, Pascal Pernot, Jamal Khatouri, and Jacqueline Belloni\*

Contribution from the Laboratoire de Chimie Physique, UMR 8000 CNRS-UPS, Bât. 349, Université Paris-Sud, 91405 Orsay Cedex, France

Received: October 10, 2000; In Final Form: February 26, 2001

The reduction mechanism of Chini clusters  $[\text{Pt}_3(\text{CO})_6]_n^{2-}$  ( $n = 6-9$ ) has been studied by nanosecond pulse radiolysis in water/2-propanol solution. The mono-electronic reduction of all  $[\text{Pt}_3(\text{CO})_6]_n^{2-}$  by the alcohol radicals produced by the solvent radiolysis is supposed to yield short-lived  $[\text{Pt}_3(\text{CO})_6]_n^{3-}$  clusters that split immediately into  $[\text{Pt}_3(\text{CO})_6]_4^{2-}$  and  $[\text{Pt}_3(\text{CO})_6]_2^{2-}$ .  $[\text{Pt}_3(\text{CO})_6]_2^{2-}$  dimerizes to the stable tetramer  $[\text{Pt}_3(\text{CO})_6]_4^{2-}$  with a diffusion-controlled rate constant. When only a fraction of the  $[\text{Pt}_3(\text{CO})_6]_n^{2-}$  in solution is reduced, a slower addition reaction between excess  $[\text{Pt}_3(\text{CO})_6]_n^{2-}$  and the newly formed  $[\text{Pt}_3(\text{CO})_6]_4^{2-}$  gives then two  $[\text{Pt}_3(\text{CO})_6]_5^{2-}$ . Results concerning the early steps of the reduction of clusters of higher nuclearity  $[\text{Pt}_3(\text{CO})_6]_n^{2-}$  ( $n = 7-9$ ) are also presented. The general reduction mechanism of the platinum carbonyl compounds  $[\text{Pt}_3(\text{CO})_6]_n^{2-}$  displays some similarities with the reduction of  $n = 6$ ; i.e., stable  $[\text{Pt}_3(\text{CO})_6]_4^{2-}$  are formed together with the transient  $[\text{Pt}_3(\text{CO})_6]_{n-4}^-$ .

## Introduction

Over the past 30 years, the interest in platinum carbonyl molecular clusters, in solution or supported, has been increasing because of the specific thermodynamic properties they display due to their small size.<sup>1-4</sup> As early as 1970, for example, the role of these platinum molecular Chini clusters  $[\text{Pt}_3(\text{CO})_6]_n^{2-}$  as catalysts was demonstrated,<sup>5-7</sup> namely for electrochemical methanol oxidation and recently as a sensitizer in photographic emulsions.<sup>8</sup> These clusters were synthesized by keeping a platinum salt in a CO-saturated basic medium for hours. Under reducing conditions, metal reduction, ligation, and aggregation reactions compete, leading to molecular clusters  $[\text{Pt}_3(\text{CO})_6]_n^{2-}$ . They display twisted prismatic structure composed of  $n$  stacking triangular units stabilized by CO ligands (bridged and linear) and a doubly negative charge (Figure 1).<sup>1</sup> The intertriangular distance is 3.08–3.10 Å for  $n = 3-6$ . It has been shown at least for the dimer that the charges are delocalized in the bonding combination of antibonding  $\pi^*$  molecular orbitals of CO and that the dianionic dimer is more stable than the neutral one.<sup>9</sup> Interesting specific redox properties of  $[\text{Pt}_3(\text{CO})_6]_n^{2-}$  have been found for these clusters ( $n = 2-10$ ).<sup>1,2,10-13</sup> The general trend in these compounds is one where the reactivity toward reducing agents increases with  $n$  and the reactivity toward oxygen increases with decreasing  $n$ . However, despite these extensive studies, no detailed reaction mechanism has been yet directly observed. Several chemical balances of redox reactions have been established, but individual reaction steps and the kinetics of these different chemical processes were never observed, and even no speculative mechanism has been proposed. Nevertheless, the mechanism of these reactions must be considered as of crucial importance for the understanding of the redox behavior of  $[\text{Pt}_3(\text{CO})_6]_n^{2-}$  clusters in catalytic reactions.

When the steady-state  $\gamma$ -irradiation of cluster solutions is carried out at room temperature and under CO atmosphere (Figure 2), the reductive process follows the sequence<sup>14</sup>

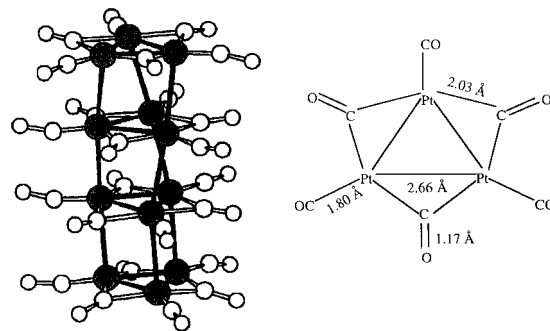
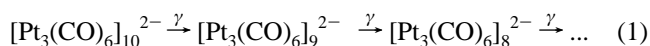


**Figure 1.** Structure of  $[\text{Pt}_3(\text{CO})_6]_n^{2-}$  Chini clusters ( $n = 4$ ). They are formed by a twisted prismatic stacking of  $n$  triangular  $\text{Pt}_3(\text{CO})_6$  units, stabilized by two negative charges. The intertriangular distance between stacked units is 3.08–3.10 Å for  $n = 3-6$ .<sup>1</sup>

The reducing species are directly produced by radiolysis of the hydro-alcohol mixed solvent. When irradiated, the 2-propanol-water solvent behaves as a strongly reducing medium due to the formation of solvated electrons  $e^-_s$  replaced by  $\text{H}^\bullet$  atoms under acidic conditions and of  $(\text{CH}_3)_2\text{C}^\bullet\text{OH}$  radicals (noted  $\text{R}^\bullet$ ). These are produced from excited alcohol molecules or by alcohol scavenging of  $\text{OH}^\bullet$  and  $\text{H}^\bullet$  radicals. The radiolytic radicals  $\text{R}^\bullet$  progressively reduce  $[\text{Pt}_3(\text{CO})_6]_{10}^{2-}$  into  $[\text{Pt}_3(\text{CO})_6]_9^{2-}$ , itself replaced after further reduction by  $[\text{Pt}_3(\text{CO})_6]_8^{2-}$ . Other clusters produced in these reactions become reactants as the radiolysis is continued.

The aim of the present study is to determine the mechanism and intermediate steps involved in the reduction of  $[\text{Pt}_3(\text{CO})_6]_n^{2-}$  clusters. Because such clusters are highly reactive, we took advantage of the time-resolved pulse radiolysis technique<sup>15,16</sup> to observe their spectral properties evolution and their reactivity. The carbonyl platinum clusters that will be studied in the present work are constituted of 6, 7, 8, or 9  $[\text{Pt}_3(\text{CO})_6]$  trigonal units. They are all stable and their optical spectra present two specific intense absorption bands in the visible range. In the red, they are at quite distinct wavelengths but in the blue the bands are very close (Figure 2).<sup>11,14</sup> Spectroscopic measurements<sup>17</sup> and

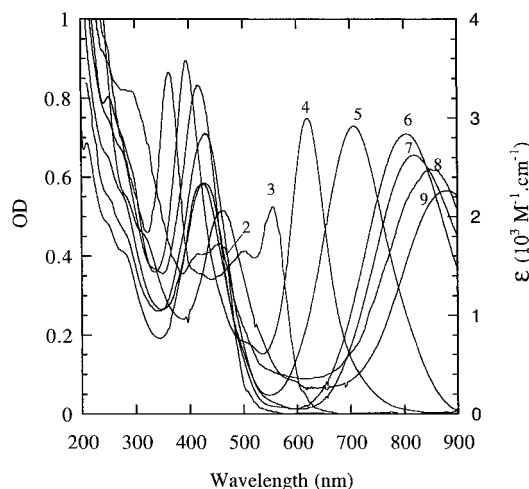
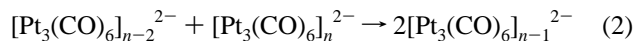


**Figure 2.** Absorption spectra of  $[\text{Pt}_3(\text{CO})_6]_{n=2-9}^{2-}$  obtained by increasing the irradiation dose.  $[\text{K}_2\text{PtCl}_4]$ :  $2.5 \times 10^{-4}$  M (in Pt atoms); (50/50% v/v  $\text{H}_2\text{O}/2\text{-PrOH}$ );  $[\text{CO}] \approx 4.7 \times 10^{-3}$  M. Dose rate:  $5 \text{ kGy} \cdot \text{h}^{-1}$ . Optical length = 1 cm. pH = 3.2. Doses: 20 kGy ( $n = 2$ ), 10 kGy ( $n = 3$ ), 3.2 kGy ( $n = 4$ ), 1.6 kGy ( $n = 5$ ), 0.8 kGy ( $n = 6$ ), 0.4 kGy ( $n = 7$ ), 0.2 kGy ( $n = 8$ ), 0.1 kGy ( $n = 9$ ). Extinction coefficients are expressed per Pt atom.

MO calculations<sup>9,18</sup> of the electronic structure of  $[\text{Pt}_3(\text{CO})_6]_n^{2-}$ . Chini clusters have shown that their absorption bands must be interpreted as the envelopes of several electronic transitions of similar energies. The first part of this work will be devoted to the mono-electronic reduction of  $[\text{Pt}_3(\text{CO})_6]_n^{2-}$  clusters (all or part of them), the second to the comparative study of clusters of higher nuclearity  $[\text{Pt}_3(\text{CO})_6]_n^{2-}$  ( $n = 7-9$ ).

## Experimental Section

Clusters  $[\text{Pt}_3(\text{CO})_6]_n^{2-}$  ( $n = 6-9$ ) were prepared by  $\gamma$ -radiolysis of  $\text{K}_2\text{PtCl}_4$  solutions at pH 3.2 under a CO atmosphere (reaction 1), as described in a previous work.<sup>14</sup> Chemicals were reagent grade and used without further purification:  $\text{K}_2\text{PtCl}_4$  from Johnson Matthey, 2-propanol from Prolabo, CO (99.995% purity) from Air Liquide. The solvent used was a 50/50 v/v water/2-propanol mixture to increase CO solubility. The dose absorbed was calculated from that in pure water and from the electronic density. The yields are estimated in a first approximation as the average between water and alcohol solution yields. Solutions containing the platinum salt ( $10^{-5}$ – $10^{-3}$  M) were carefully saturated with carbon monoxide under 1 atm. Such solutions were then exposed to a  $^{60}\text{Co}$  source (dose rate  $1.6 \text{ kGy h}^{-1}$ ) at various irradiation doses depending on the nuclearity  $n$  desired. Indeed, the radiolytic synthesis is selective and  $n$  is controlled by adjusting the dose (the higher the dose, the lower the  $n$  value:  $0.1 \text{ kGy}/(\text{mmol L}^{-1})$  for  $n = 9$ ,  $0.4 \text{ kGy mM}^{-1}$  for  $n = 8$ ,  $0.6 \text{ kGy mM}^{-1}$  for  $n = 7$ , or  $0.8 \text{ kGy mM}^{-1}$  for  $n = 6$ ) (Figure 2). Actually, the clusters of nuclearity  $n-2$  which are produced by reduction of  $n-1$  would readily recombine with excess clusters with nuclearity  $n$  as in



The selectivity of the radiolytic synthesis with the dose is due to this reaction between clusters of nonconsecutive nuclearities, already described in the literature.<sup>2</sup>

Since the clusters are highly reactive with oxygen, the solutions were handled, after the synthesis by  $\gamma$ -radiolysis, in a

glovebox under an inert atmosphere of  $\text{N}_2$ . Samples of the solutions were placed in optical cells for identification and for time-resolved experiments in the absence of CO. The nuclearity was deduced from the very specific UV/vis absorption spectra recorded on a VARIAN DMS 100 Instrument. The pulsed radiolysis facility (3 ns at half-height and 600 keV electron energy), the flow cell flushed with nitrogen (perpendicular optical length = 1 cm), and the time-resolved optical detection have been described elsewhere.<sup>19</sup> Doses per pulse vary from less than 0.1 kGy to 0.3 kGy. They are obtained from dosimetry in water with the hydrated electron signal and from the relative electron density of the 2-propanol–water mixture. After each pulse, the irradiated sample is replaced by fresh solution. The time range of observation starts after the end of the pulse (10 ns) and, due to diffusion in the cell, was limited to 40 s.

In experiments with pulsed irradiation, the reduction process is initiated as in  $\gamma$ -radiolysis. After an electron pulse, the solvated electrons  $e^-_s$  are readily exhausted within  $\sim 200$  ns and replaced by  $\text{H}^\bullet$  radicals, because the main reactant  $\text{H}^+$  at pH 3.2 is in large excess relative to the clusters. As soon as they are formed, the  $\text{H}^\bullet$  radicals produced (also by direct radiolysis of  $\text{H}_2\text{O}$  and alcohol) are scavenged by 2-propanol as well as  $\text{OH}^\bullet$  radicals arising from water radiolysis. Therefore, the  $(\text{CH}_3)_2\text{C}^\bullet\text{OH}$  radical (noted  $\text{R}^\bullet$ ) is the only reducing species reacting with  $[\text{Pt}_3(\text{CO})_6]_n^{2-}$ . The radical yield is estimated to be  $G(\text{R}^\bullet) \sim 5$ , from the interpolated value between those in acidic aqueous solutions of 2-propanol ( $G = 6$ ) and in neat 2-propanol ( $G \sim 4$ ). The neat mechanism observed is a reduction of clusters. Therefore, we exclude a possible oxidizing role of these radicals in the present case. Under pulse conditions, the instantaneous radical  $\text{R}^\bullet$  concentration is in large excess relative to  $[\text{Pt}_3(\text{CO})_6]_n^{2-}$ , in contrast with steady-state radiolysis, and the radicals that do not reduce the clusters  $[\text{Pt}_3(\text{CO})_6]_n^{2-}$  disproportionate and dimerize without further effect.

The kinetic schemes have been tested by global least-squares fitting<sup>20</sup> against the experimental time-resolved absorption spectra after the pulse irradiation. At each wavelength, the optical density  $\text{OD}(\lambda, t)$  is  $\text{OD}(\lambda, t) = \sum \epsilon_i(\lambda) c_i(t)$ . The unknown molecular extinction coefficients of transients  $\epsilon_i(\lambda)$  were determined independently for each species  $i$ . The instantaneous concentrations  $c_i(t)$  were calculated by adaptive step size fourth-order Runge–Kutta integration of the kinetic equations.<sup>21</sup> Unknown rate constants have been allowed to vary in the global fitting procedure. Very short time reactions (electron scavenging by  $\text{H}^+$ , alcohol radical formation) have not been explicitly taken into account in our kinetic schemes. As a consequence, the fitting procedure excludes times below 500–1000 ns, and the  $\text{R}^\bullet$  initial (around 1 ms) concentration is adjusted.

## Results and Discussion

**$[\text{Pt}_3(\text{CO})_6]_6^{2-}$  Solutions.** The initial solution studied by pulse radiolysis contains  $[\text{Pt}_3(\text{CO})_6]_6^{2-}$  at  $1.25 \times 10^{-4}$  to  $2.5 \times 10^{-4}$  M (in Pt atom) or  $0.7 \times 10^{-5}$  to  $1.4 \times 10^{-5}$  M (in cluster) in an equivolumic 2-propanol/water mixture under acid conditions (pH = 3.2) and  $\text{N}_2$  atmosphere.  $[\text{Pt}_3(\text{CO})_6]_6^{2-}$  clusters present two specific narrow absorption bands at 430 and 802 nm (Figure 2). The extinction coefficients are  $\epsilon_{802} = 5.14 \times 10^4$  and  $\epsilon_{430} = 5.04 \times 10^4 \text{ M}^{-1} \text{ cm}^{-1}$  per cluster, respectively.<sup>10</sup>

**One-Electron Reduction of All the Clusters.** Figure 3 shows the time evolution of spectra in the microsecond range, recorded when a solution containing  $[\text{Pt}_3(\text{CO})_6]_6^{2-}$  at  $2.5 \times 10^{-4}$  M (in

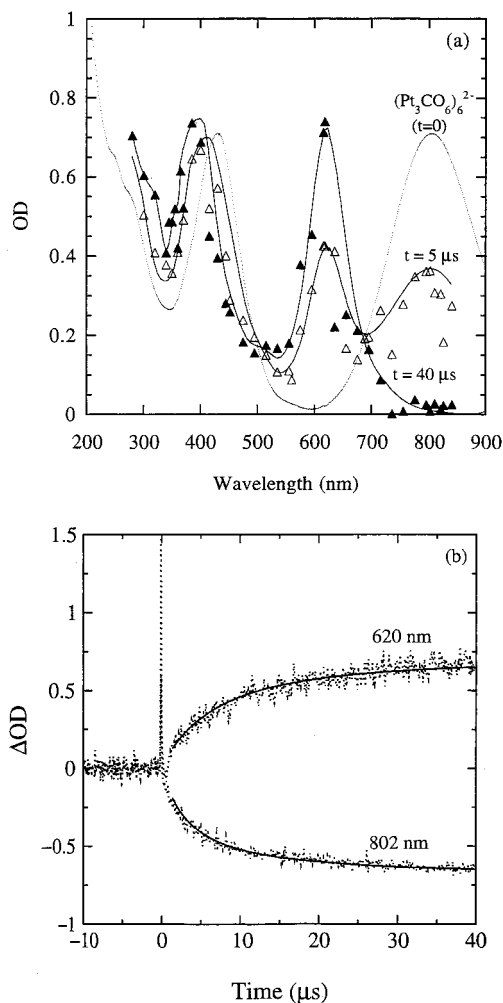
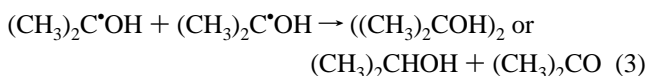


**Figure 3.** (a) Evolution of the absorption spectra of a solution of  $[\text{Pt}_3(\text{CO})_6]_6^{2-}$  from  $t = 0$  (before the pulse) to  $t = 5 \mu\text{s}$  and  $t = 40 \mu\text{s}$  after the pulse. Total mono-electronic reduction. Spectra deduced from  $\text{OD}(\lambda) = \Delta\text{OD}_t(\lambda) + \text{OD}_{t=0}(\lambda)$ .  $[[\text{Pt}_3(\text{CO})_6]_6^{2-}] = 1.4 \times 10^{-5} \text{ M}$  ( $[\text{Pt}] = 2.5 \times 10^{-4} \text{ M}$ );  $\text{pH} = 3.2$ ; (50/50% v/v  $\text{H}_2\text{O}/2\text{-PrOH}$ ). Dose rate  $\sim 0.3 \text{ kGy/pulse}$ . (b). Correlated signals (dashed lines) at  $\lambda = 802 \text{ nm}$  and  $\lambda = 620 \text{ nm}$  with a single pulse and the corresponding fitting (lines). The initial very fast formation and decay are due to the short-lived solvated electron ( $\lambda_{\text{max}}$  close to  $730 \text{ nm}$ ). Values adjusted by the simulation at  $t > 1 \text{ ms}$ :  $[\text{R}^*]_{1\mu\text{s}} = 1.4 \times 10^{-4} \text{ M}$ ,  $k_4 = 1.85 \times 10^9 \text{ M}^{-1} \text{ s}^{-1}$ ,  $k_5 > 10^{11} \text{ s}^{-1}$ ,  $2k_6 = 2.4 \times 10^{10} \text{ M}^{-1} \text{ s}^{-1}$ .

Pt atoms) or  $1.4 \times 10^{-5} \text{ M}$  (in clusters) was irradiated with a dose per pulse of approximately  $0.28 \text{ kGy}$ , equivalent to a concentration of radicals  $[\text{R}^*] \sim 1.4 \times 10^{-4} \text{ M}$ . These spectra were obtained by addition of the experimental differential spectra ( $\Delta\text{OD}_t(\lambda)$ ) at 5 or 40 ms and of the initial optical density ( $\text{OD}_{t=0}(\lambda)$ ) of  $[\text{Pt}_3(\text{CO})_6]_6^{2-}$ :  $\text{OD}_t(\lambda) = \Delta\text{OD}_t(\lambda) + \text{OD}_{t=0}(\lambda)$ . Since alcohol radicals are formed at  $t \sim 500 \text{ ns}$ , but they only absorb in the UV, they do not affect the visible spectrum of the  $[\text{Pt}_3(\text{CO})_6]_6^{2-}$  clusters before irradiation at 802 and 430 nm. Note that in contrast to the  $\gamma$ -radiolysis (reaction 1), the alcohol radicals are formed within a short time and, if not reacted with the clusters, they disproportionate and dimerize readily:

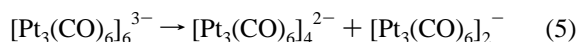
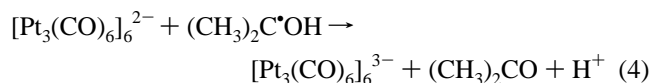


( $2k_3 = (1.56 \pm 0.10) \times 10^9 \text{ M}^{-1} \text{ s}^{-1}$  in pure water).<sup>22</sup>

However, the 802 nm band decreases (bleaching) and a new band at 620 nm progressively appears a few milliseconds after

the irradiation (Figure 3). The  $[\text{Pt}_3(\text{CO})_6]_6^{2-}$  clusters have entirely disappeared from the solution at 40 ms, as shown by the complete bleaching of the 802 nm absorption band. A spectrum recorded at the end of the reaction has two very intense bands at 395 and 620 nm, which indicate the presence of stable clusters with  $n = 4$ ,  $[\text{Pt}_3(\text{CO})_6]_4^{2-}$  (Figures 2 and 3a). From the optical density at 620 nm and the extinction coefficient  $\epsilon_{620}([\text{Pt}_3(\text{CO})_6]_4^{2-}) = 3.6 \times 10^4 \text{ M}^{-1} \text{ cm}^{-1}$  per cluster, the estimated concentration of the  $[\text{Pt}_3(\text{CO})_6]_4^{2-}$  cluster formed per pulse is  $2.05 \times 10^{-5}$  or  $2.5 \times 10^{-4} \text{ M}$  in Pt atom, and thus equal to the initial atom concentration of  $[\text{Pt}_3(\text{CO})_6]_6^{2-}$ . Therefore, it is clear that  $[\text{Pt}_3(\text{CO})_6]_6^{2-}$  clusters (oxidation degree  $-2/18$ ) have been quantitatively replaced by  $[\text{Pt}_3(\text{CO})_6]_4^{2-}$  ( $-2/12 = -3/18$ ) clusters. This process corresponds exactly to a mono-electronic reduction. The presence of quasi-isosbestic points at 500 and 690 nm suggests that other possible transients formed in the mechanism have lifetimes much shorter than the microsecond range or are under minor concentrations.

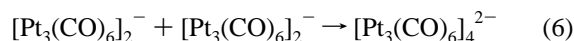
Figure 3b shows the typical time evolution profiles of the differential absorbance at  $\lambda = 802 \text{ nm}$  and  $\lambda = 620 \text{ nm}$  obtained after the same pulse. The initial very fast formation and decay are due to the short-lived solvated electron ( $\lambda_{\text{max}}$  close to  $730 \text{ nm}$ ). Then the  $[\text{Pt}_3(\text{CO})_6]_4^{2-}$  formation at 620 nm is correlated to the absorption decay at 802 nm. However,  $[\text{Pt}_3(\text{CO})_6]_4^{2-}$  cannot be stoichiometrically produced from  $[\text{Pt}_3(\text{CO})_6]_6^{2-}$  by the one-electron reduction without a rearrangement of atoms. One or several intermediates must be formed prior to the appearance of the product. The decay of  $[\text{Pt}_3(\text{CO})_6]_6^{2-}$  and the increase of  $[\text{Pt}_3(\text{CO})_6]_4^{2-}$  both obey the same apparent second-order kinetic law. We suppose that  $\text{R}^*$  radicals first reduce  $[\text{Pt}_3(\text{CO})_6]_6^{2-}$  into the triply charged clusters  $[\text{Pt}_3(\text{CO})_6]_6^{3-}$ , which split immediately into  $[\text{Pt}_3(\text{CO})_6]_4^{2-}$  and  $[\text{Pt}_3(\text{CO})_6]_2^{-}$ :



An alcohol radical-cluster complex is possibly formed as a transient in the reduction reaction (4). However, no spectral evidence of  $[\text{Pt}_3(\text{CO})_6]_6^{3-}$  was found in our spectra. Unstable  $[\text{Pt}_3(\text{CO})_6]_6^{3-}$  splits as in (5) without being detected. Though suggested by the material balance, triply charged clusters such as  $[\text{Pt}_3(\text{CO})_6]_6^{3-}$  and mono-charged clusters such as  $[\text{Pt}_3(\text{CO})_6]_2^{-}$  have never been spectrally identified in the literature, probably owing to their high reactivity and their transient character.

Because the initial concentration of clusters,  $1.4 \times 10^{-5} \text{ M}$ , is much lower than the  $(\text{CH}_3)_2\text{C}^{\bullet}\text{OH}$  radical concentration,  $(1-2) \times 10^{-4} \text{ M}$  per pulse, reaction 4 competes with the  $(\text{CH}_3)_2\text{C}^{\bullet}\text{OH}$  disproportionation/dimerization (3).<sup>22</sup>

Because of this competition, the decay of  $[\text{Pt}_3(\text{CO})_6]_6^{2-}$  is indeed kinetically close to second order. Nevertheless, the amount of  $[\text{Pt}_3(\text{CO})_6]_4^{2-}$  formed indicates that, at this dose rate, all clusters  $[\text{Pt}_3(\text{CO})_6]_6^{2-}$  have received one electron from  $(\text{CH}_3)_2\text{C}^{\bullet}\text{OH}$  radicals (reaction 4). Following reaction 5,  $[\text{Pt}_3(\text{CO})_6]_2^{-}$  clusters dimerize into stable tetramers:



Numerical simulation of the mechanism (reactions 3-6), included the value of  $k_3$ , which was taken as equal to the literature value in pure water.<sup>22</sup> The simulation also assumed

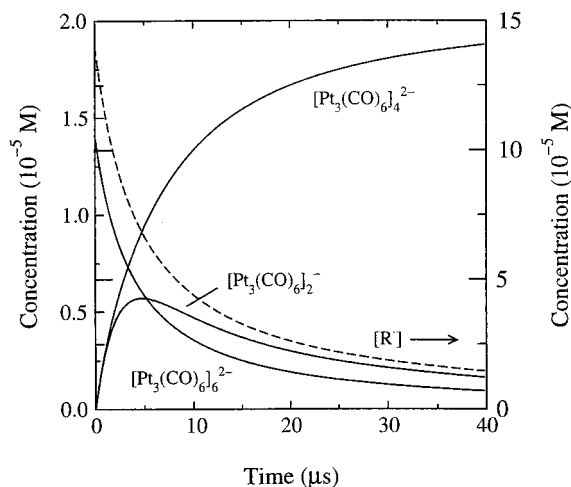


**Figure 4.** Kinetic profiles of cluster and alcohol radical concentrations obtained from the simulation under the experimental conditions and with rate constants as in Figure 3.

that reaction 5 was very fast. Calculations were made for a series of radical concentrations that accounted for signals measured at different doses per pulse (0.2–0.4 kGy) and different  $[\text{Pt}_3(\text{CO})_6]_6^{2-}$  concentrations ( $(0.7\text{--}1.4) \times 10^{-5}$  M).

A fit of experimental to calculated signals is shown as an example for  $[\text{R}^*] = 1.4 \times 10^{-4}$  M in Figure 3b. Note that  $[\text{Pt}_3(\text{CO})_6]_6^{3-}$  and  $[\text{Pt}_3(\text{CO})_6]_2^-$  are consumed as soon as formed, due to the high values of  $k_5$  and  $k_6$ , respectively. Thus, the optical density of both species at 802 and 620 nm have little influence on the calculated signal whatever the values of their extinction coefficients. The adjusted values are  $k_4 = 1.85 \times 10^9 \text{ M}^{-1} \text{ s}^{-1}$ ,  $k_5 > 10^{11} \text{ s}^{-1}$ , and  $2k_6 = 2.4 \times 10^{10} \text{ M}^{-1} \text{ s}^{-1}$ , independently of the dose per pulse, i.e., of the initial concentration of alcohol radicals. Time profiles of cluster and  $\text{R}^*$  concentrations are given in Figure 4. The reduction (4) by the alcohol radical is over within 20–30  $\mu\text{s}$  and is the time-limiting step. It appears that the dimerization (6) is fast enough to maintain the  $[\text{Pt}_3(\text{CO})_6]_2^-$  concentration at a small level and to enable a correlation between the decay at 802 nm of the initial cluster  $[\text{Pt}_3(\text{CO})_6]_6^{2-}$  during the reduction and the increase at 620 nm of stable  $[\text{Pt}_3(\text{CO})_6]_4^{2-}$ , with the presence of quasi-isosbestic points at 500 and 690 nm. The one-electron reduction process (reactions 4–6) corresponds to an integral overall transformation of hexamers into tetramers.

**One-Electron Reduction of Part of  $[\text{Pt}_3(\text{CO})_6]_6^{2-}$ .** To study the effect of the reducing species concentration on the kinetics, a fraction only of  $[\text{Pt}_3(\text{CO})_6]_6^{2-}$  was reduced by decreasing the irradiation dose delivered per pulse ( $\leq 0.16$  kGy). The concentration of radicals is now about  $\leq 0.7 \times 10^{-4} \text{ mol L}^{-1}$ . In the nanosecond and microsecond range, we observed the same reduction of  $[\text{Pt}_3(\text{CO})_6]_6^{2-}$  into  $[\text{Pt}_3(\text{CO})_6]_4^{2-}$ . Nevertheless, the reduction of  $[\text{Pt}_3(\text{CO})_6]_6^{2-}$  was quantitatively less important because most of the radicals disappear by dimerization (3) rather than by reaction (4). The spectrum of nonreduced  $[\text{Pt}_3(\text{CO})_6]_6^{2-}$  is still present at 80 ms, as expected (Figure 5a), but additional spectral changes are observed at the millisecond scale. Beyond a few milliseconds, the specific bands of remaining  $[\text{Pt}_3(\text{CO})_6]_6^{2-}$  and of newly formed  $[\text{Pt}_3(\text{CO})_6]_4^{2-}$  simultaneously decrease and two new bands appear in the final optical spectrum at 705 and around 410 nm (Figure 5a,b), which correspond to clusters of nuclearity  $n = 5$ ,  $[\text{Pt}_3(\text{CO})_6]_5^{2-}$  (Figure 2). Therefore, the spectral change observed at 1–10 ms is assigned to the formation of  $[\text{Pt}_3(\text{CO})_6]_5^{2-}$  clusters through an addition reaction of type (2) between the nonconsecutive  $[\text{Pt}_3(\text{CO})_6]_6^{2-}$  and  $[\text{Pt}_3(\text{CO})_6]_4^{2-}$  cluster chains (reaction 7) followed by the

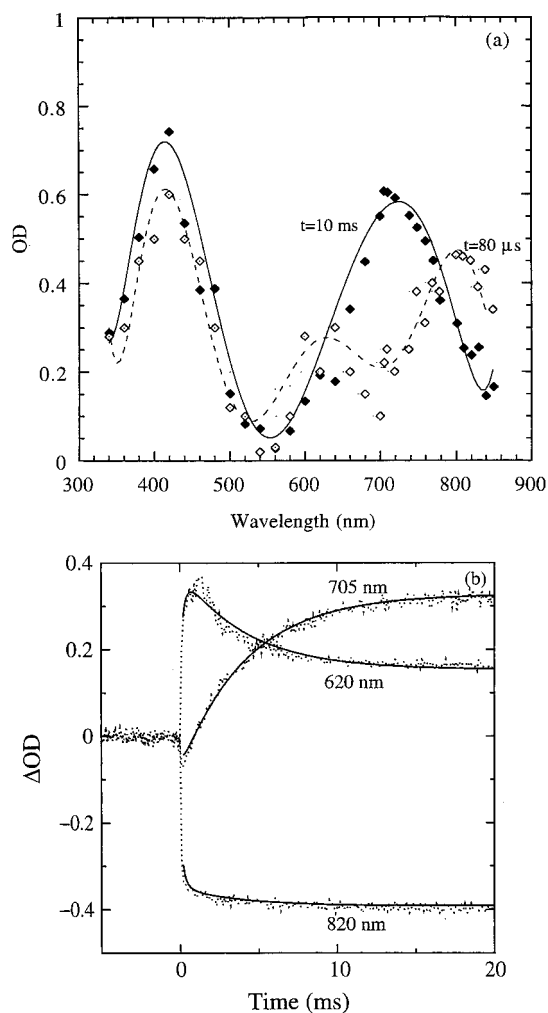
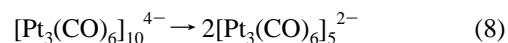
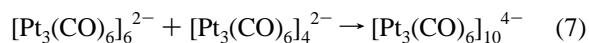


**Figure 5.** (a) Evolution of the absorption spectra of a solution of  $[\text{Pt}_3(\text{CO})_6]_6^{2-}$  at  $t = 80 \mu\text{s}$  and  $t = 10$  ms after a pulse. Monoelectronic reduction of part of clusters. Spectra deduced from  $\text{OD}(\lambda) = \Delta\text{OD}(\lambda) + \text{OD}_{t=0}(\lambda)$ .  $[\text{R}^*]_{1\mu\text{s}} = 1 \times 10^{-5}$  M. Other conditions and initial spectrum at  $t = 0$  as in Figure 3. (b). Correlated signals at  $\lambda = 802$  nm,  $\lambda = 620$  nm, and  $\lambda = 705$  nm at the millisecond range after a pulse and their corresponding fitting.  $k_4$  and  $k_6$  as in Figure 3a.  $[\text{R}^*]_{1\mu\text{s}} = 5 \times 10^{-6}$  M,  $k_7 = 6 \times 10^8 \text{ M}^{-1} \text{ s}^{-1}$ , and  $k_8 = 3 \times 10^2 \text{ s}^{-1}$ .

cleavage (8) of  $[\text{Pt}_3(\text{CO})_6]_{10}^{4-}$  into smaller oligomers:



It corresponds indeed to an electron-transfer reaction between a small and a heavier cluster, resulting in clusters of intermediate size.

A reaction between nonconsecutive clusters ( $n \leq 6$ ,  $\Delta n \geq 2$ ) is known to produce clusters of intermediate nuclearity,<sup>2</sup> as demonstrated by mixing two solutions containing  $[\text{Pt}_3(\text{CO})_6]_n^{2-}$  and  $[\text{Pt}_3(\text{CO})_6]_{n+2}^{2-}$  clusters. However, the kinetics were never investigated up to now. The relative concentrations of both species govern the final composition of the solution. Indeed, if  $R = [[\text{Pt}_3(\text{CO})_6]_{n+2}^{2-}]/[[\text{Pt}_3(\text{CO})_6]_n^{2-}] > 1$ , a mixture of  $[\text{Pt}_3(\text{CO})_6]_{n+2}^{2-}$  and  $[\text{Pt}_3(\text{CO})_6]_{n+1}^{2-}$  is obtained. By contrast,  $[\text{Pt}_3(\text{CO})_6]_n^{2-}$  and  $[\text{Pt}_3(\text{CO})_6]_{n+1}^{2-}$  coexist in the solution if  $R < 1$ . In our experiments, the ratio  $R$  depends on the concentration of  $[\text{Pt}_3(\text{CO})_6]_4^{2-}$  generated after the electron pulse and on the remaining concentration of  $[\text{Pt}_3(\text{CO})_6]_6^{2-}$ , and thus on the irradiation dose per pulse. According to the concentration values

calculated from the transient spectrum obtained at 80 ms (Figure 5a),  $R > 1$ .  $[\text{Pt}_3(\text{CO})_6]_5^{2-}$  and a slight excess of  $[\text{Pt}_3(\text{CO})_6]_6^{2-}$  are thus present and coexist at the end in the solution in the molar relation established by the dose.

Numerical simulations under partial reducing conditions included the rate constants  $k_4$  to  $k_6$  with their above determined values (under reduction of all the clusters). A satisfying fit is obtained between experimental and calculated values up to 500 ms, but departures are observed in the range  $10^{-3}$ – $10^{-2}$  s when the new reactions 7 and 8 are included in the mechanism and the splitting of  $[\text{Pt}_3(\text{CO})_6]_{10}^{4-}$  clusters (reaction 8) is assumed very fast. The calculated absorbance would be too small at 820 nm and too large at 620 nm for any value of  $k_7$ , even if signals fit eventually rather well at  $10^{-2}$ – $10^{-1}$  s with the material balance. This suggests that the  $[\text{Pt}_3(\text{CO})_6]_{10}^{4-}$  splitting should be slow enough to let it somewhat accumulate up to a detectable level and that  $[\text{Pt}_3(\text{CO})_6]_{10}^{4-}$  absorbs strongly at 620 nm. The best fitting (Figure 5b) is obtained with  $\epsilon_{620} = 6.0 \times 10^4 \text{ M}^{-1} \text{ cm}^{-1}$ ,  $\epsilon_{820} = 3.3 \times 10^4 \text{ M}^{-1} \text{ cm}^{-1}$ , and  $\epsilon_{705} = 2.4 \times 10^4 \text{ M}^{-1} \text{ cm}^{-1}$  per cluster. In this mechanism, it is found that  $k_7 = 6 \times 10^8 \text{ M}^{-1} \text{ s}^{-1}$  and  $k_8 = 3 \times 10^2 \text{ s}^{-1}$ . The relative slowness of (7) is probably due to a possible reverse dissociation of  $[\text{Pt}_3(\text{CO})_6]_{10}^{4-}$  into the same initial stable clusters  $[\text{Pt}_3(\text{CO})_6]_6^{2-}$  and  $[\text{Pt}_3(\text{CO})_6]_4^{2-}$ .

Although some examples of such a reaction between two nonconsecutive clusters are known in chemistry, this time-resolved study of the process has allowed us to observe it directly for the first time and to evaluate the rate constant in the case of the reaction of  $[\text{Pt}_3(\text{CO})_6]_6^{2-}$  with  $[\text{Pt}_3(\text{CO})_6]_4^{2-}$ .

**Comparison with  $\gamma$ -Radiolysis.** When  $[\text{Pt}_3(\text{CO})_6]_6^{2-}$  are reduced by  $\gamma$ -radiolysis, the alcohol radicals are produced very slowly in accordance with the low dose rate. Therefore, all radicals are scavenged by the clusters (reaction 4) and the recombination (3) becomes negligible. Tetramers formed in (5) and (6) react also progressively with nonreduced  $[\text{Pt}_3(\text{CO})_6]_6^{2-}$  (reactions 7 and 8), so that the pentamer  $[\text{Pt}_3(\text{CO})_6]_5^{2-}$  eventually accumulates, at least for doses up to 0.8 kGy under the same concentration condition ( $2.5 \times 10^{-4}$  M in Pt atoms) as above. Further irradiation of  $[\text{Pt}_3(\text{CO})_6]_5^{2-}$  leads quantitatively to  $[\text{Pt}_3(\text{CO})_6]_4^{2-}$  through a mechanism similar to the hexamer mechanism (reactions 3–8), but initiated now by the splitting of the reduced form of the pentamer  $[\text{Pt}_3(\text{CO})_6]_5^{3-}$ .

The slowness of the  $\gamma$ -induced reduction of  $[\text{Pt}_3(\text{CO})_6]_6^{2-}$  by the radicals allows the accumulation of  $[\text{Pt}_3(\text{CO})_6]_5^{2-}$  after a transient formation of  $[\text{Pt}_3(\text{CO})_6]_4^{2-}$ , as observed by pulse radiolysis under conditions where only a fraction of the initial  $[\text{Pt}_3(\text{CO})_6]_6^{2-}$  clusters are reduced.

**$[\text{Pt}_3(\text{CO})_6]_{7-9}^{2-}$  Solutions.** The one-electron reduction of each cluster in solutions of  $[\text{Pt}_3(\text{CO})_6]_n^{2-}$ , with  $n = 7-9$ , under various conditions of concentration of clusters ( $6 \times 10^{-6}$  to  $1.5 \times 10^{-5}$  M) and radicals ( $[\text{R}^*] = \text{a few } 10^{-4}$  M) was accomplished by following the procedure of preceding experiments.

**$[\text{Pt}_3(\text{CO})_6]_7^{2-}$  Solutions.** The first step observed at nanosecond scale with  $[\text{Pt}_3(\text{CO})_6]_7^{2-}$  solutions ( $1.2 \times 10^{-5}$  M in cluster) is, as shown above, the solvated electron scavenging by hydronium ions. This reaction must be followed sequentially by the rapid formation of alcohol radicals and the reaction of  $(\text{CH}_3)_2\text{C}^*\text{OH}$  with  $[\text{Pt}_3(\text{CO})_6]_7^{2-}$ . The disappearance of  $[\text{Pt}_3(\text{CO})_6]_7^{2-}$  clusters is observed at the maximum wavelengths, 820 and 425 nm, while absorbances at 620 nm and at 560 nm increase at the same time scale. The process is over within 80 ms (Figure 6a). The new absorption band at 620 nm corresponds clearly to clusters of nuclearity  $n = 4$  (Figure 2). Note that at

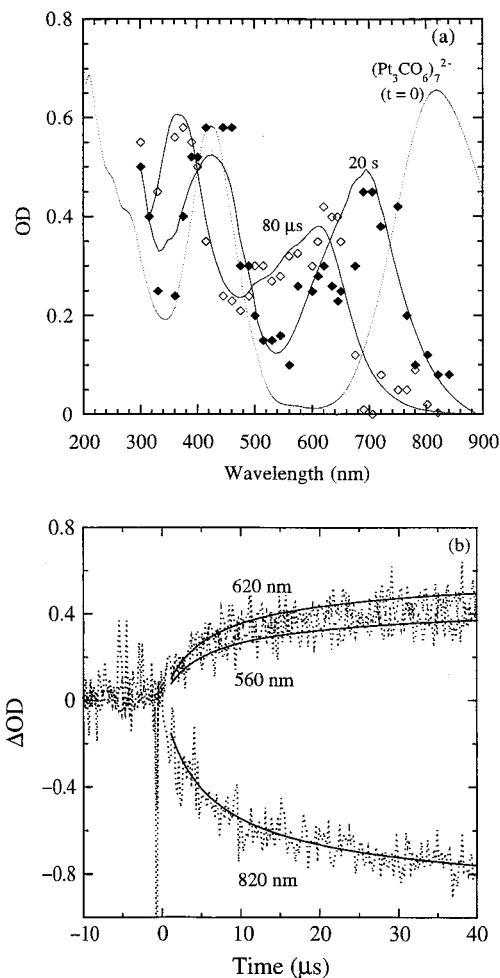
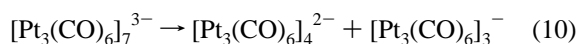
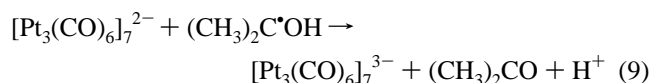


**Figure 6.** (a) Absorption spectra of a solution of  $[\text{Pt}_3(\text{CO})_6]_7^{2-}$  at  $t = 80 \mu\text{s}$  and  $t = 20$  s after a pulse.  $[[\text{Pt}_3(\text{CO})_6]_7^{2-}] = 1.2 \times 10^{-5}$  M ( $[\text{Pt}] = 2.5 \times 10^{-4}$  M). Other conditions as in Figure 3. (b). Correlated signals at  $\lambda = 705$  nm,  $\lambda = 560$  nm, and  $\lambda = 620$  nm after a pulse.  $[[\text{Pt}_3(\text{CO})_6]_7^{2-}] = 1.85 \times 10^{-5}$  M ( $[\text{Pt}] = 3.8 \times 10^{-4}$  M). Adjusted values:  $[\text{R}^*]_{1\mu\text{s}} = 2.0 \times 10^{-4}$  M,  $k_9 = 8.6 \times 10^8 \text{ M}^{-1} \text{ s}^{-1}$ .

560 nm the absorbance is much higher than in the  $[\text{Pt}_3(\text{CO})_6]_4^{2-}$  spectrum. Therefore, additional species are present. From the balance, the splitting of the reduced form  $[\text{Pt}_3(\text{CO})_6]_7^{3-}$  should indeed lead to the doubly charged  $[\text{Pt}_3(\text{CO})_6]_4^{2-}$  and the simply charged  $[\text{Pt}_3(\text{CO})_6]_3^-$ :

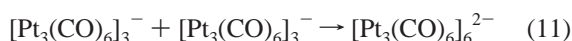


The maximum and the intensity of the simply charged  $[\text{Pt}_3(\text{CO})_6]_3^-$  absorption band is apparently close to that of the doubly charged trimer, at least around 560 nm. Alcohol radicals concomitantly disappear by reaction 3.

Numerical simulations for various dose conditions give, as it was indicated above, the time evolution of the total absorbance at different wavelengths (560, 620, and 820 nm) in the microsecond range. The splitting (10) being assumed very fast, the adjusted value is  $k_9 = 8.6 \times 10^8 \text{ M}^{-1} \text{ s}^{-1}$  (Figure 6b).

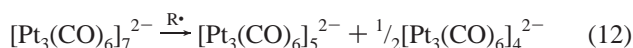
At the millisecond scale, no change is observed in the absorption spectra, while at longer times ( $\sim 20$  s), the decay of absorbances at 560 and 620 nm is observed, and simultaneously an absorption increase occurs at 705 and 420 nm, which is

assigned to the formation of  $[\text{Pt}_3(\text{CO})_6]_5^{2-}$  clusters (Figure 6a). The most likely mechanism is that  $[\text{Pt}_3(\text{CO})_6]_3^-$  clusters dimerize into  $[\text{Pt}_3(\text{CO})_6]_6^{2-}$ :



and that a further reaction of  $[\text{Pt}_3(\text{CO})_6]_6^{2-}$  just formed in reaction (11) with  $[\text{Pt}_3(\text{CO})_6]_4^{2-}$  yields  $[\text{Pt}_3(\text{CO})_6]_5^{2-}$  as shown above in reactions 7 and 8. Accounting for the values determined for  $k_7$  and  $k_8$ , the adjusted value is  $2k_{11} = 3 \times 10^4 \text{ M}^{-1} \text{ s}^{-1}$ .

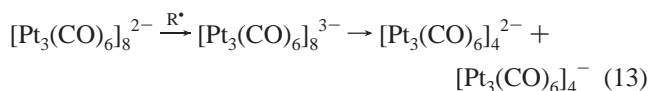
The reduction process of clusters of nuclearity  $n = 7$  is therefore similar to that observed for  $[\text{Pt}_3(\text{CO})_6]_6^{2-}$  in the preceding section. The cluster reduction is followed by a splitting reaction and leads to molecular clusters of smaller nuclearities, in particular,  $[\text{Pt}_3(\text{CO})_6]_4^{2-}$ .  $[\text{Pt}_3(\text{CO})_6]_5^{2-}$  is then formed very slowly by reaction between  $[\text{Pt}_3(\text{CO})_6]_6^{2-}$  and  $[\text{Pt}_3(\text{CO})_6]_4^{2-}$ . The final spectrum corresponds to a one-electron reduction of all initial clusters  $n = 7$  into  $n = 5$  and  $n = 4$  (which do not react together) according to the overall balance:



This material balance implies that a possible reduction of  $[\text{Pt}_3(\text{CO})_6]_3^-$  by the alcohol radicals does not occur under the conditions of the experiment.

$[\text{Pt}_3(\text{CO})_6]_{n=8,9}^{2-}$  Solutions. The reduction of  $[\text{Pt}_3(\text{CO})_6]_8^{2-}$  and  $[\text{Pt}_3(\text{CO})_6]_9^{2-}$  was also studied in order to check whether the above mechanism of  $[\text{Pt}_3(\text{CO})_6]_n^{2-}$  reduction, namely the systematic formation of  $[\text{Pt}_3(\text{CO})_6]_4^{2-}$ , is general to clusters of higher  $n$  value.

For  $n = 8$ , an absorbance increase is observed at 620 nm only and is correlated with the decay of  $[\text{Pt}_3(\text{CO})_6]_8^{2-}$  at 852 nm (Figure 7a). The band at 620 nm is assigned as above to tetramers. The final absorbance at 620 nm and the initial one at 852 nm are close and according to Figure 2 correspond to an integral reduction of octamers into tetramers. But, because of the material balance, the  $[\text{Pt}_3(\text{CO})_6]_8^{3-}$  splitting leads to both doubly and monocharged tetramers:



Then, no change is observed from 40  $\mu\text{s}$  to 40 s. It is unlikely that the monocharged tetramer  $[\text{Pt}_3(\text{CO})_6]_4^-$  is so long-lived. Therefore, a further reduction of this species by excess alcohol radicals should be assumed to occur:



In the simulation (where the  $[\text{Pt}_3(\text{CO})_6]_8^{2-}$  reduction is also in competition with reaction 3), the absorbances of both tetramers at 620 nm are supposed to be close, and it is found that  $k_{13} = 7.2 \times 10^8 \text{ M}^{-1} \text{ s}^{-1}$ . Note that the process (13)–(14) corresponds indeed to an overall reduction of two electrons per  $[\text{Pt}_3(\text{CO})_6]_8^{2-}$  cluster, leading to two tetramers.

For  $n = 9$ , we observed also the formation of  $[\text{Pt}_3(\text{CO})_6]_4^{2-}$  at 620 nm and, in addition, a band at 705 nm. The increases in the absorbances are correlated with the decay at 875 nm due to the  $[\text{Pt}_3(\text{CO})_6]_9^{2-}$  reduction in competition with (3).

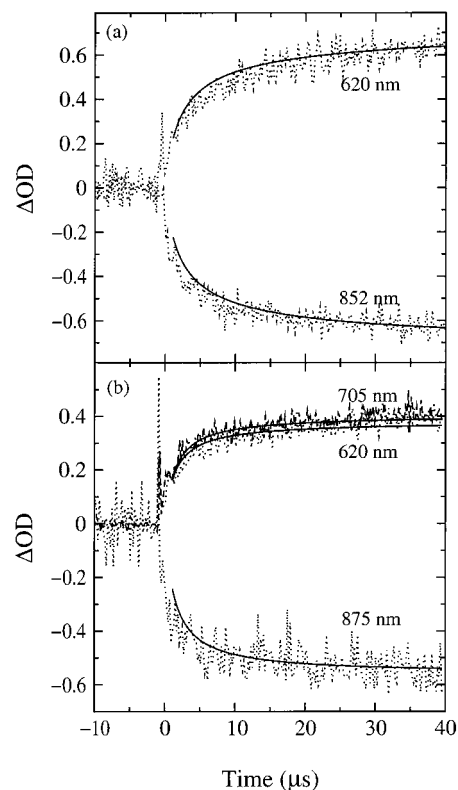
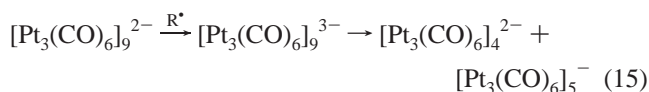
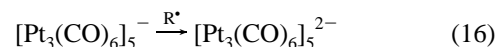


**Figure 7.** (a) Correlated signals at  $\lambda = 852 \text{ nm}$  and  $\lambda = 620 \text{ nm}$  with a single pulse.  $[[\text{Pt}_3(\text{CO})_6]_8^{2-}] = 1.1 \times 10^{-5} \text{ M}$  ( $[\text{Pt}] = 2.5 \times 10^{-4} \text{ M}$ ). Other conditions as in Figure 3. Values adjusted by simulation:  $[\text{R}^*]_{1\mu\text{s}} = 6.3 \times 10^{-4} \text{ M}$ ,  $k_{13} = 7.2 \times 10^8 \text{ M}^{-1} \text{ s}^{-1}$ . (b). Correlated signals at  $\lambda = 875 \text{ nm}$ ,  $\lambda = 705 \text{ nm}$ , and  $\lambda = 620 \text{ nm}$  with a single pulse.  $[[\text{Pt}_3(\text{CO})_6]_9^{2-}] = 9.5 \times 10^{-6} \text{ M}$  ( $[\text{Pt}] = 2.5 \times 10^{-4} \text{ M}$ ). Adjusted values:  $[\text{R}^*]_{1\mu\text{s}} = 5.3 \times 10^{-4} \text{ M}$ ,  $k_{15} = 1.3 \times 10^9 \text{ M}^{-1} \text{ s}^{-1}$ .

Then, at least up to 40 s (limit of observation), no decay was observed at 620 and 705 nm. As stated above, it is improbable that  $[\text{Pt}_3(\text{CO})_6]_5^-$  could be stable so long. Seemingly,  $[\text{Pt}_3(\text{CO})_6]_5^-$  is also reduced by excess radicals  $\text{R}^*$  into  $[\text{Pt}_3(\text{CO})_6]_5^{2-}$ .



The reaction kinetics have been simulated (Figure 7b) and the rate constant of reaction 15 is  $k_{15} = 1.3 \times 10^9 \text{ M}^{-1} \text{ s}^{-1}$ . The final absorbances at 620 and 705 nm compared to the initial one at 875 nm correspond indeed to the balance of the mechanism (15)–(16). The overall bielectronic reduction of  $[\text{Pt}_3(\text{CO})_6]_9^{2-}$  leads to stable consecutive tetramers and pentamers that do not react mutually, as in the heptamer reduction.

## Conclusion

The mechanism of the slow reduction (by a chemical agent or by  $\gamma$ -radiolysis) of platinum carbonyl clusters  $[\text{Pt}_3(\text{CO})_6]_n^{2-}$ , results in a decrease of the cluster nuclearity  $n$  by one unit from  $[\text{Pt}_3(\text{CO})_6]_n^{2-}$  to  $[\text{Pt}_3(\text{CO})_6]_{n-1}^{2-}$ . The present pulse radiolysis observations show for the first time that the mechanism involves in fact a sequence initiated by a mono-electronic transfer from the reducing agent. The reaction steps and kinetics involved in the process of multistep rearrangement of the trigonal units were directly investigated. These time-resolved observations of the irradiated solutions demonstrate that the reduction process of clusters  $[\text{Pt}_3(\text{CO})_6]_{n=6-9}^{2-}$  presents general features. Whether  $n$  is odd or even, the process starts by a mono-electronic transfer from alcohol radicals and yields  $[\text{Pt}_3(\text{CO})_6]_n^{3-}$  with a rate constant of  $(0.7 \text{ to } 1.8) \times 10^9 \text{ M}^{-1} \text{ s}^{-1}$ . These species are

unstable and split immediately into  $[\text{Pt}_3(\text{CO})_6]_4^{2-}$  and  $[\text{Pt}_3(\text{CO})_6]_{n-4}^-$ . Then the fate of unstable  $[\text{Pt}_3(\text{CO})_6]_{n-4}^-$  depends on the nuclearity  $n$ . The smallest ones ( $n = 6$  or  $7$ ) dimerize; the other ones ( $n = 8$  or  $9$ ) are easily reduced. The dimerization rate constants of  $[\text{Pt}_3(\text{CO})_6]_2^{2-}$  and  $[\text{Pt}_3(\text{CO})_6]_3^-$  (to yield  $[\text{Pt}_3(\text{CO})_6]_4^{2-}$  and  $[\text{Pt}_3(\text{CO})_6]_6^{2-}$ , respectively) were determined. In contrast, the reduction of  $[\text{Pt}_3(\text{CO})_6]_4^-$  and  $[\text{Pt}_3(\text{CO})_6]_5^-$  by excess radicals into  $[\text{Pt}_3(\text{CO})_6]_4^{2-}$  and  $[\text{Pt}_3(\text{CO})_6]_5^{2-}$ , respectively, is much faster than their dimerization, probably owing to an increase of the cluster reduction potential with the nuclearity as in the doubly charged cluster series.

The pulse radiolysis study under reduction conditions of only part of  $[\text{Pt}_3(\text{CO})_6]_6^{2-}$  also enables the observation of the reaction occurring between two nonconsecutive oligomers, such as  $n = 4$  and  $n = 6$ , yielding pentamers, which is a consequence of the redox potential increase with the nuclearity. This indicates that the mechanism in the steady-state regime of  $\gamma$ -radiolytic reduction of  $[\text{Pt}_3(\text{CO})_6]_6^{2-}$  is indeed a multistep process that yields the doubly charged tetramer as a transient species before the formation of  $[\text{Pt}_3(\text{CO})_6]_5^{2-}$ . Similar multistep mechanisms have to be assumed also for slow reduction of other nuclearities.

Generally, the observations have shown that reduced transient clusters  $[\text{Pt}_3(\text{CO})_6]_n^{3-}$ , or oxidized ones  $[\text{Pt}_3(\text{CO})_6]_n^-$  could be formed, indicating that the platinum molecular clusters could thus act either as electron donors or as acceptors depending on the reactant.

**Acknowledgment.** We are indebted to AGFA-Gevaert N. V. Co, for financial support.

## References and Notes

(1) Calebrese, J. C.; Dahl, L. F.; Chini, P.; Longoni, G.; Martinengo, S. *J. Am. Chem. Soc.* **1974**, *96*, 2614.

- (2) Longoni, G.; Chini, P. *J. Am. Chem. Soc.* **1976**, *98*, 7225.  
 (3) Chini, P. *J. Organomet. Chem.* **1980**, *200*, 37.  
 (4) Yamamoto, T.; Shido, T.; Inagaki, S.; Fukushima, Y.; Ichikawa, M. *J. Phys. Chem. B* **1998**, *102*, 3866, and references therein.  
 (5) Li, Guang-Jin.; Fujimoto, T.; Fukuoka, A.; Ichikawa, M. *Catal. Lett.* **1992**, *12*, 171.  
 (6) Le Gratiot, B.; Remita, H.; Picq, G.; Delcourt, M. O. *J. Catal.* **1996**, *164*, 36.  
 (7) Torigoe, K.; Remita, H.; Picq, G.; Belloni, J.; Bazin, D. *J. Phys. Chem. B* **2000**, *104*, 7050.  
 (8) De Keyzer, R.; Treguer, M.; Remita, H.; Belloni, J. AGFA G. V. Patent, US 09/159, 225, Sept 23, 1998.  
 (9) Underwood, J.; Hoffman, R.; Tatsumi, K.; Nakamura, A.; Yamamoto, Y. *J. Am. Chem. Soc.* **1985**, *107*, 5968.  
 (10) Cerriotti, A.; Longoni, G.; Marchionna, M. *Inorg. Synth.* **1990**, *26*, 316.  
 (11) D'Aniello, M. J.; Carr, C. J.; Zammit, G. *Inorg. Synth.* **1990**, *26*, 319.  
 (12) Fujimoto, T.; Fukuoka, A.; Ichikawa, M. *Chem. Mater.* **1992**, *4*, 104.  
 (13) Fujimoto, T.; Fukuoka, A.; Iijima, S.; Ichikawa, M. *J. Phys. Chem.* **1993**, *97*, 279.  
 (14) Le Gratiot, B.; Remita, H.; Picq, G.; Delcourt, M. O. *Radiat. Phys. Chem.* **1996**, *47*, 263.  
 (15) Baxendale, J. H.; Busi, F., Eds. *The Study of Fast Processes and Transient Species by Electron Pulse Radiolysis*; NATO ASI Vol. 86; Reidel: Dordrecht, The Netherlands, 1982.  
 (16) Tabata, Y.; Ito, Y.; Tagawa, S., Eds. *Handbook of Radiation Chemistry*; CRC Press: Boca Raton, FL, 1991.  
 (17) Roginski, R. T.; Shapley, J. R.; Drickamer, H. G.; D'Aniello, M. *J. Chem. Phys. Lett.* **1987**, *135*, 525.  
 (18) Woolley, R. G. *Chem. Phys. Lett.* **1988**, *143*, 145.  
 (19) Belloni, J.; Billiau, F.; Delaire, J. A.; Delcourt, M. O.; Marignier, J. L. *Radiat. Phys. Chem.* **1983**, *21*, 177.  
 (20) Beechem, J. M.; Ameloot, M.; Brand, L. *Chem. Phys. Lett.* **1985**, *120*, 466.  
 (21) Press, W. H.; Teukolsky, S. A.; Vetterling, W. T.; Flannery B. P. *Numerical Recipes*, 2nd ed.; Cambridge University Press: Cambridge, U. K., 1992.  
 (22) Mezyk, S. P.; Madden, K. P. *J. Phys. Chem. A* **1999**, *103*, 235.